

Outcome-guided Bayesian Clustering for Disease Subtype Discovery Using High-dimensional Transcriptomic Data

Lingsong Meng, Zhiguang Huo *

Department of Biostatistics, University of Florida

Abstract

The discovery of disease subtypes is an essential step for developing precision medicine, and disease subtyping via omics data has become a popular approach. While promising, subtypes obtained from conventional approaches may not be necessarily associated with clinical outcomes. The collection of rich clinical data along with omics data has provided an unprecedented opportunity to facilitate the disease subtyping process and to discovery clinically meaningful disease subtypes. Thus, we developed an outcome-guided Bayesian clustering (GuidedBayesianClustering) method to fully integrate the clinical data and the high-dimensional omics data. A Gaussian mixed model framework was applied to perform sample clustering; a spike-and-slab prior was utilized to perform gene selection; a mixture model prior was employed to incorporate the guidance from a clinical outcome variable; and a decision framework was adopted to infer the false discovery rate of the selected genes. We deployed conjugate priors to facilitate efficient Gibbs sampling. Our proposed full Bayesian method is capable of simultaneously (i) obtaining sample clustering (disease subtype discovery); (ii) performing feature selection (select genes related to the disease subtype); and (iii) utilizing clinical outcome variable to guide the disease subtype discovery. The superior performance of the GuidedBayesianClustering was demonstrated through simulations and applications of breast cancer expression data.

Keywords: Outcome-guided clustering, Bayesian method, Gaussian mixed model, Gibbs sampling

1 Introduction

Many complex diseases are difficult to treat because of the large amount of variabilities among the affected patients, and the personalized medicine is a promising approach because of its potential to deliver the most responsive and effective therapy (Vogenberg et al., 2010). One of the most challenging and daunting tasks

*Correspondence: Z.H. zhuo@ufl.edu

for developing personalized medicine is to perform disease subtyping – identifying subgroups of patients with similar pathological conditions. With the rapid advancement of high-throughput technology, disease subtyping via molecular data (e.g., gene expression data) is becoming increasingly popular, which has been applied to many diseases including lymphoma (Rosenwald et al., 2002), glioblastoma (Parsons et al., 2008; Verhaak et al., 2010), breast cancer (Lehmann et al., 2011; Parker et al., 2009), colorectal cancer (Sadanandam et al., 2013), ovarian cancer (Tothill et al., 2008), Parkinson’s disease (Williams-Gray and Barker, 2017) and Alzheimer’s disease (Bredesen, 2015).

Taking breast cancer as an example, Parker et al. (2009) developed 50 gene signatures (a.k.a PAM50) that classified breast cancer into five molecular subtypes, including Luminal A, Luminal B, Her2-enriched, Basal-like and Normal-like. These subtypes had shown distinct disease mechanisms, treatment responses and, survival outcomes (Van’t Veer et al., 2002; Coates et al., 2015). For example, the Luminal A subtype has the best prognosis, the HER2-enriched subtype can be treated by Herceptin, and the Basal-like subtype is considered to have the worst survival. The clinical value of these breast cancer molecular subtypes were further appreciated by clinical trial studies (Von Minckwitz et al., 2012; Prat et al., 2015).

Unsupervised clustering methods, which aim to partition a dataset into several distinct subgroups, are effective ways to perform disease subtyping. In the literature, several classical clustering methods have been employed for this purpose, including hierarchical clustering (Eisen et al., 1998), K -means (Dudoit and Fridlyand, 2002), mixture model-based approaches (McLachlan et al., 2002). These classical clustering methods were particularly successful when the data is in low dimension (i.e., large number of samples and small number of genes). Modern transcriptomic studies usually have tens of thousands of genes, and it is generally assumed that only a small subset of genes are related to the disease subtypes. To accommodate this issue, sparse clustering algorithms were proposed to simultaneously select the intrinsic genes and perform sample clustering. Along this direction, Witten and Tibshirani (2010) proposed a sparse Kmeans algorithm. In their paper, instead of assuming equal contribution of each gene feature that was used in the classical Kmeans, they designed a weighted Kmeans and imposed l_1/l_2 norm penalties on the gene weights. In their algorithm, the penalty would result in zero weights for many non-informative genes, and genes with non-zero weights were treated as selected genes. Similarly, Pan and Shen (2007); Xie et al. (2008) proposed to impose a weight penalization on the Gaussian mixture models. Bouveyron and Brunet-Saumard (2014) provided a review for high-dimensional model-based clustering.

While these methods were successful in obtaining results for both clustering and gene selection, there are still limitations. It is well acknowledged that clustering algorithms are sensitive to initializations and can be trapped in local optimum solutions. Such local optimum problems can be further amplified in the case of high-dimensional data. For high-dimensional data, people have noticed the existence of multi-facet

clusters (Gaynor and Bair, 2017; Nowak and Tibshirani, 2008), where multiple configurations of sample clusters defined by separated gene sets may co-exist in the same dataset. These multiple configurations could be driven by genes associated with age, sex, and other confounding variables or pathological processes, rather than the intrinsic genes (i.e., genes related to the underlying disease). We utilized the METABRIC data – a breast cancer gene expression profile to illustrate the concept of the multi-facet clusters. This METABRIC data was also used in the later real data application (See Section 3.2 for detailed description about this dataset). Since age, estrogen receptor (ER), human epidermal growth factor receptor 2 (Her2), and progesterone receptor (PR) were hallmarks of the Breast cancer, we first pre-selected the top 100 significant age-related, ER-related, HER2-related, or PR-related genes via univariate regression. Then, for each set of these pre-selected genes (e.g., top 100 ER-related genes), we extracted these genes from the high-dimensional gene expression profile as features, and performed sample clustering using the classical Kmeans. This analysis was performed for each of these 4 sets of pre-mentioned breast cancer related genes, respectively. Figure 1A showed that the subtype patterns obtained by different sets of pre-selected genes were quite distinct. Figure 1B assessed the clustering agreement via ARI (See Section 3 for definitions). The pairwise ARI ranged from 0.14 \sim 0.47, indicating poor to moderate clustering agreement among configurations from different gene sets. Figure 1C compared the gene selection agreement via Jaccard index (See Section 3 for definitions). The pairwise Jaccard indexes ranged from 0.00 \sim 0.29, indicating poor gene selection agreement among clustering configurations from different gene sets. Collectively, Figure 1 demonstrated the existence of multi-facet clusters (distinct clustering configurations driven by different gene sets). Therefore, without specifying disease-related genes, a clustering algorithm is likely to identify a subtype configuration that optimizes its objective function. However, the resulting subtype may not be clinically meaningful, and the selected genes may not be biologically relevant.

In modern biomedical studies, comprehensive clinical data are routinely collected. Some of these information could be quite relevant to the underlying disease, and thus, properly incorporating such prior knowledge could potentially facilitate the identification of disease-related clustering configuration. In the literature, several clustering methods have been proposed to incorporate prior knowledge. Basu et al. (2004) proposed a constrained clustering algorithm by forcing/forbidding two samples in a cluster according to prior knowledge. Huo et al. (2017) proposed an overlapping group lasso penalty to incorporate prior biological pathway information for a clustering algorithm. However, these algorithms still could not ensure the resulting subtypes to be related to the underlying disease. Bair and Tibshirani (2004) proposed a two-step semi-supervised clustering methods, where they pre-selected a list of disease-related genes, and then performed the regular Kmeans. Though this algorithm emphasized that the selected genes were related to the disease, the algorithm could not promise that these selected genes were capable of minimizing within

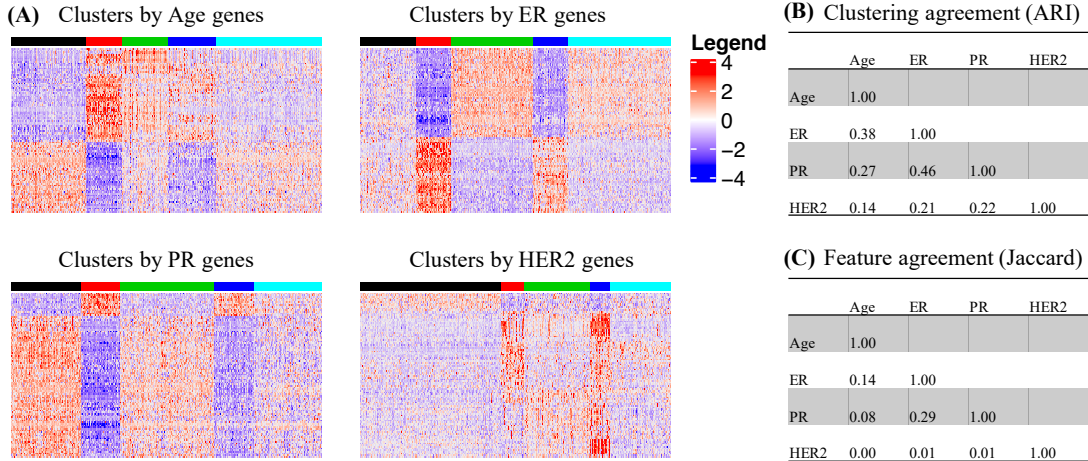


Figure 1: Illustrating of multi-facet clusters defined by different genes. In (A), top 100 age-related, ER-related, PR-related, or HER2-related genes were used to perform clustering analysis, respectively. In the heatmap, each row represents a gene, and each column represents a sample. Within a heatmap, the samples under the same color bar represents the samples from the same cluster. (B) shows the pairwise cluster agreement among clustering results guided by different clinical variables. (C) shows the pairwise gene selection agreement among clustering results guided by different clinical variables.

cluster dispersions. In other word, the resulting subtypes could render large within group variability because the selected genes could carry large variability, which would make it difficult to predict a future patient. In addition, they adopted an arbitrary cutoff to define their pre-selected genes, which may require further justifications in real data applications.

To address these existing limitations, we propose a full Bayesian hierarchical model to identify subtypes in a high-dimensional data, which will simultaneously (i) obtain sample clustering (disease subtype discovery); (ii) perform gene selection (select genes related to the disease subtype); and (iii) incorporate the guidance of a clinical outcome variable. Utilizing disease-related clinical outcome guidance will encourage the identification of disease-related subtypes from the many configurations (multi-facet clusters) defined by other confounding genes. In our model, a Gaussian mixture model framework is applied to perform sample clustering; a spike and slab prior is used for gene selection; a mixture model prior is employed to incorporate the guidance of a clinical outcome variable; and a decision framework is established to infer the false discovery rate of the selected genes. Our full Bayesian framework has the advantage of providing a probabilistic belief of feature selection as well as soft assignment of cluster labels instead of a hard-thresholding approach. The priors are designed to be fully conjugate to facilitate efficient Gibbs sampling. Our approach utilizes non-informative priors as much as possible such that the process of subtype identification process is data driven. We evaluated the performance of our method in simulations and real data applications, and demonstrated its superior performance in comparison with regular sparse Bayesian approach (without guidance term). An

R package has been made publicly available on GitHub to improve the applicability of our method.

2 Method

2.1 Gaussian mixture model

Denote X_{gi} as the gene expression level of gene g ($1 \leq g \leq G$) for the sample i ($1 \leq i \leq n$), where G is total number of genes and n is total number of samples. We assume the gene expression matrix is properly standardized such that for each gene g , $\mathbf{x}_g = (X_{g1}, \dots, X_{gn})^\top$ has mean 0 and standardization 1.

Denote Z_i as a subtype indicator, with $Z_i = k$ indicating sample i belongs to subtype k ($1 \leq k \leq K$), where K is total number of subtypes. The scalar form $Z_i = k$ is equivalent to the vector form $Z_i = (0, \dots, 0, 1, 0, \dots, 0)^\top$, where 1 appears at the k^{th} position. We will use these two forms interchangeably when there is no ambiguity.

By assuming (i) the gene expression data comes from a Gaussian mixture model, and (ii) genes are independent with each other, we have

$$X_{gi} \sim N(\mu_{gk}, \sigma_g^2) | Z_i = k$$

$$Z_i \sim \text{Mult}(1; \pi_1, \dots, \pi_K),$$

where μ_{gk} is the mean expression level of gene g in subtype k ; σ_g^2 is variance of the expression level of gene g . Mult denotes the multinomial distribution; π_k is the proportion of subtype k and $\sum_{k=1}^K \pi_k = 1$;

Under the Gaussian mixture model, the complete likelihood function for the observed data $\mathbf{X} = \{X_{gi}\}_{i=1, \dots, n; g=1, \dots, G}$ and subtype indicator $\mathbf{Z} = \{Z_i\}_{i=1, \dots, n}$ is:

$$L(\Theta | \mathbf{X}, \mathbf{Z}) = \prod_{i=1}^n \prod_{k=1}^K \left[\pi_k \prod_{g=1}^G \frac{1}{\sqrt{2\pi}\sigma_g} \exp \left\{ -\frac{(X_{gi} - \mu_{gk})^2}{2\sigma_g^2} \right\} \right]^{I(Z_i=k)}$$

where Θ presents all unknown parameters including π_k , μ_{gk} and σ_g^2 ($1 \leq k \leq K$, $1 \leq g \leq G$), and $I(\cdot)$ is an indicator function with $I(\cdot) = 1$ if the expression inside (\cdot) is true and 0 otherwise.

2.2 Sparse Gaussian mixture model

Biologically, it is acknowledged that only a small subset of intrinsic genes will contribute to the final subtyping result. Recall that each gene has been standardized (i.e., $\sum_i X_{gi} = 0$). Since an intrinsic gene should well separate different clusters, its cluster centers should be away from 0; while a non-intrinsic gene could not

well separate different clusters, thus all of its cluster centers should be close to 0. We denote L_g as the gene selection indicator, with $L_g = 1$ indicating gene g is selected, and $L_g = 0$ indicating gene g is not selected. We denote p as the prior probability of $L_g = 1$. To achieve gene selection, we assume a spike-and-slab (Ishwaran et al., 2005) prior for μ_{gk} :

$$\mu_{gk} \sim \text{N}(0, \tau_{\mu 1}^2) | L_g = 1;$$

$$\mu_{gk} \sim \text{N}(0, \tau_{\mu 0}^2) | L_g = 0;$$

$$L_g \sim \text{Bernoulli}(p),$$

where $\tau_{\mu 1}^2$ is the variance of the intrinsic genes, and $\tau_{\mu 0}^2$ is the variance of the non-intrinsic genes. If $\tau_{\mu 1}^2 > \sigma_0^2$ ($\sigma_0^2 > 0$ is some positive number) and $\tau_{\mu 0}^2 \rightarrow 0$, then $\mu_{gk} | L_g = 1$ is likely to be non-zero and $\mu_{gk} | L_g = 0$ is likely to be close to 0. By imposing this spike-and-slab prior, genes with large separation ability are likely to be selected (i.e., $L_g = 1$). We will discuss how to specify $\tau_{\mu 1}^2$ and $\tau_{\mu 0}^2$ in section 2.3.3. Such modeling strategy has been previously described by Luo and Wei (2019).

2.3 Guided Bayesian Clustering

2.3.1 Motivation of using mixture model priors to incorporate clinical outcome guidance

We hypothesize that a disease-related clinical variable has the potential to improve gene selection in a sparse clustering algorithm. To be specific, the intrinsic genes are more likely to be associated with the clinical variable than the non-intrinsic genes. To examine this hypothesis, we first calculated the absolute values of the correlation coefficient ($\boldsymbol{\rho} = (\rho_1, \dots, \rho_G)^\top$) between a clinical variable (i.e., Estrogen receptor) and all gene features based on the METABRIC data (see Section 3.2 for more details about this dataset). To obtain the intrinsic genes, we applied the sparse Kmeans algorithm (with initialized weights proportional to $\boldsymbol{\rho}$), and defined intrinsic genes as the top 400 genes with the largest gene selection weights. As shown in Figure 2, the mean ρ (in absolute value) in the selected genes group is 0.40, which is much higher than that of the non-selected genes group (0.16), with $p \leq 2.2 \times 10^{-16}$. This implies that we could potentially use these association strengths with respect to a clinical variable to facilitate gene selections.

In general, we propose to use a gene specific guiding term U_g to represent the association strength between gene g and a clinical outcome variable. For example, $U_g = U(\mathbf{x}_g, \mathbf{y})$, where $\mathbf{x}_g = (X_{g1}, \dots, X_{gn})^\top \in \mathbb{R}^n$ is the expression levels of gene g , and $\mathbf{y} = (y_1, \dots, y_n)^\top \in \mathbb{R}^n$ is the vector of a clinical outcome variable. Under this definition, ρ_g is a special case of U_g when function U represents the absolute value of the correlation coefficient. For the ease of modeling, we design the association strength $\mathbf{u} = (U_1, \dots, U_G)^\top$ to range from (0,1). More discussion of the design on \mathbf{u} is available in Section 2.3.7.

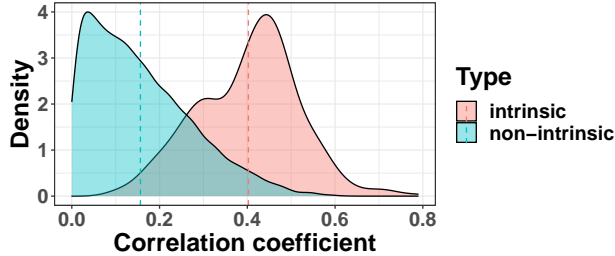


Figure 2: Correlation coefficient distribution (absolute value) among intrinsic (selected) genes and non-intrinsic genes. Dashed lines represent the mean correlation. The mean correlation for the intrinsic genes is 0.40, while the mean correlation for the non-intrinsic genes is 0.16.

Motivated by Figure 2, we propose to model \mathbf{u} using a mixture model approach. To be specific, we assume the distribution of \mathbf{u} is a mixture of two components. For the intrinsic genes, the distribution of \mathbf{u} follows F_1 , and for the non-intrinsic genes, the distribution of \mathbf{u} follows F_0 . Beta mixture model or Gaussian mixture model are good candidates for this purpose. To improve identifiability, we further impose a mean parameter shift between F_0 and F_1 to ensure $\mathbb{E}(F_1) > \mathbb{E}(F_0)$. For the convenience of Gibbs sampling, we adopt a Gaussian mixture model with mean parameter 0 for F_0 and mean parameter 1 for F_1 throughout our manuscript. This design will encourage that larger U_g is more likely associated with $L_g = 1$, and smaller U_g is more likely associated with $L_g = 0$. This part can be further extended to other mixture models as needed. The Gaussian mixture model prior for U_g is shown below:

$$U_g \sim N(1, \tau_{U_1}^2) | L_g = 1;$$

$$U_g \sim N(0, \tau_{U_0}^2) | L_g = 0,$$

where $\tau_{U_1}^2$ is the variance parameter for the association strength of the intrinsic gene component (i.e., $L_g = 1$) and $\tau_{U_0}^2$ is the variance parameter for the association strength of the non-intrinsic gene component (i.e., $L_g = 0$). The selection of $\tau_{U_1}^2$ and $\tau_{U_0}^2$ will be discussed in Section 2.3.3. Such a mixture model will encourage the selection of genes that are highly associated with the clinical outcome variable.

2.3.2 Full Bayesian model

Figure 3 shows the graphical model representation of the data generative process of our Bayesian latent hierarchical model. Our model is consisted of three major components. (i) The right component, including Z_i , X_{gi} , μ_{gk} , and σ_g^2 , represents the Gaussian mixture model introduced in Section 2.1. This component is responsible for inferring the clustering results (i.e., Z_i). (ii) The middle component, including L_g , μ_{gk} , $\tau_{\mu_0}^2$ and $\tau_{\mu_1}^2$, represents the spike-and-slab prior introduced in Section 2.2. This component is responsible for

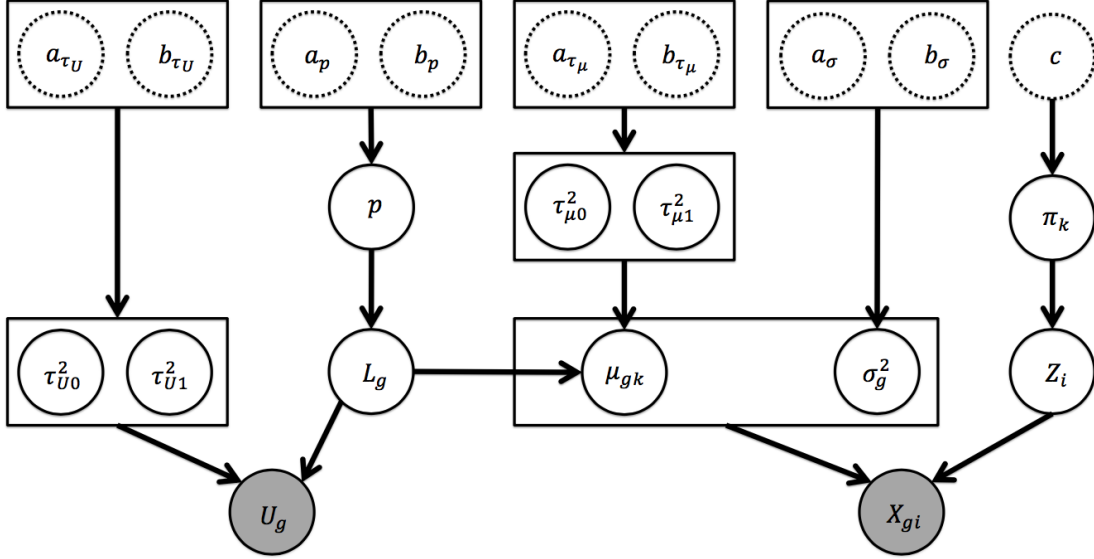


Figure 3: Graphical model representation of Bayesian latent hierarchical model. Shaded nodes are observed variables. Dashed nodes are pre-fixed hyper parameters. Arrows represent generative process. $g(1 \leq g \leq G)$ is the gene index, $i(1 \leq i \leq n)$ is the sample index, and $k(1 \leq k \leq K)$ is the subtype index.

performing gene selection (i.e., select genes with large separation ability). (iii) The left component, including L_g , U_g , τ_{U0}^2 and τ_{U1}^2 , represents the mixture model prior introduced in Section 2.3.1. This component is responsible for incorporating clinical outcome information to facilitate the disease subtyping process. The parameters of interest Θ include μ_{gk} , σ_g^2 , L_g , Z_i , p , π_k , $\tau_{\mu0}^2$, $\tau_{\mu1}^2$, τ_{U0}^2 , τ_{U1}^2 , where $1 \leq k \leq K$, $1 \leq g \leq G$. By inferring Θ from this full Bayesian model, we will simultaneously (i) obtain sample clustering result; (ii) select genes with strong separation ability; and (iii) utilize a clinical outcome variable to enhance gene selection and sample clustering.

Based on this graphical model, the full posterior likelihood $L(\Theta|\mathbf{X}, \mathbf{u})$ is proportional to:

$$\begin{aligned}
& \prod_{i=1}^n \prod_{k=1}^K \left[\pi_k \prod_{g=1}^G \frac{1}{\sqrt{2\pi}\sigma_g} \exp \left\{ -\frac{(X_{gi} - \mu_{gk})^2}{2\sigma_g^2} \right\} \right]^{I(Z_i=k)} \\
& \cdot \prod_{g=1}^G [\text{N}(U_g; 1, \tau_{U1}^2) \cdot L_g + \text{N}(U_g; 0, \tau_{U0}^2) \cdot (1 - L_g)] \\
& \cdot \prod_{g=1}^G \prod_{k=1}^K [\text{N}(\mu_{gk}; 0, \tau_{\mu1}^2) \cdot L_g + \text{N}(\mu_{gk}; 0, \tau_{\mu0}^2) \cdot (1 - L_g)] \\
& \cdot \prod_{g=1}^G [\text{Inv}\Gamma(\sigma_g^2; a_\sigma, b_\sigma) \cdot p^{L_g} (1-p)^{1-L_g}] \cdot \text{Beta}(p; a_p, b_p) \cdot \text{Dir}(\boldsymbol{\pi}; \mathbf{c}) \\
& \cdot \text{Inv}\Gamma(\tau_{\mu1}^2; a_{\tau_{\mu1}}, b_{\tau_{\mu1}}) \cdot \text{Inv}\Gamma(\tau_{\mu0}^2; a_{\tau_{\mu0}}, b_{\tau_{\mu0}}) \cdot \text{Inv}\Gamma(\tau_{U1}^2; a_{\tau_{U1}}, b_{\tau_{U1}}) \cdot \text{Inv}\Gamma(\tau_{U0}^2; a_{\tau_{U0}}, b_{\tau_{U0}}),
\end{aligned}$$

where some of the priors and hyper parameters were introduced in the following sections.

2.3.3 Prior Specification

We apply independent conjugate priors to each component in Θ as follows: $\boldsymbol{\pi} = (\pi_1, \dots, \pi_K)^\top \sim \text{Dir}(\mathbf{c})$; $\sigma_g^2 \sim \text{Inv}\Gamma(a_\sigma, b_\sigma)$; $p \sim \text{Beta}(a_p, b_p)$; $\tau_{\mu 1}^2 \sim \text{Inv}\Gamma(a_{\tau_{\mu 1}}, b_{\tau_{\mu 1}})$; $\tau_{\mu 0}^2 \sim \text{Inv}\Gamma(a_{\tau_{\mu 0}}, b_{\tau_{\mu 0}})$; $\tau_{U 1}^2 \sim \text{Inv}\Gamma(a_{\tau_{U 1}}, b_{\tau_{U 1}})$; $\tau_{U 0}^2 \sim \text{Inv}\Gamma(a_{\tau_{U 0}}, b_{\tau_{U 0}})$. Such design of conjugate priors will greatly facilitate efficient implementations of Gibbs sampling. Here, $\mathbf{c} = (c, \dots, c)^\top \in \mathbb{R}^K$, $a_\sigma, b_\sigma, a_p, b_p, a_{\tau_{\mu 1}}, b_{\tau_{\mu 1}}, a_{\tau_{\mu 0}}, b_{\tau_{\mu 0}}, a_{\tau_{U 1}}, b_{\tau_{U 1}}, a_{\tau_{U 0}}$ and $b_{\tau_{U 0}}$ are hyper parameters.

2.3.4 Hyper parameter justification

We propose to assign non-informative prior wherever possible. For instance, we will set $c = 1$; $a_p = b_p = 1$; $a_\sigma = b_\sigma = 0.001$; $a_{\tau_{U 0}} = b_{\tau_{U 0}} = 0.001$; $a_{\tau_{U 1}} = b_{\tau_{U 1}} = 0.001$. In order to distinguish intrinsic genes and non-intrinsic genes (make them identifiable), we set a_{τ_μ} and b_{τ_μ} to be informative. To be specific, we will set $a_{\tau_{\mu 0}} = 2$, $b_{\tau_{\mu 0}} = 0.005$, which will result in a small prior mean for $\tau_{\mu 0}^2$; $a_{\tau_{\mu 1}} = 4$, $b_{\tau_{\mu 1}} = 450$, which will result in large prior mean for $\tau_{\mu 1}^2$. The justification for these informative hyper parameters will be done by sensitivity analysis (see Section 3.1.3). We use the Bayesian information criterion (BIC) (Schwarz et al., 1978) to choose the number of subtypes K . The BIC formula for the GuidedBayesianClustering is (Schwarz et al., 1978) is

$$-2 \left[\sum_{i=1}^n \log \left(\sum_{k=1}^K \hat{\pi}_k \prod_{g=1}^G \text{N}(X_{gi}; \hat{\mu}_{gk}, \hat{\sigma}_g^2) \right) \right] + KG \log G,$$

where the first term is negative two times the log likelihood; the second term is the product of the parameter number and the logarithm of number of genes; $\hat{\pi}_k, \hat{\mu}_{gk}$ and $\hat{\sigma}_g^2$ are the posterior mean estimates. The number of subtypes K is chosen with the minimum BIC.

2.3.5 Posterior Calculation

We develop a Gibbs sampler algorithm to draw samples (Geman and Geman, 1984; Robert and Casella, 2013) for Θ . To be specific, in each Gibbs sampling iteration, we update one parameter in Θ while conditioning on all other parameters at their most recently updated value. The order for updating the parameter is fixed as $p, \tau_{\mu 0}^2, \tau_{\mu 1}^2, \tau_{U 0}^2, \tau_{U 1}^2, L_g, \boldsymbol{\pi}, Z_i, \mu_{gk}, \sigma_g^2$, where $1 \leq k \leq K$ and $1 \leq g \leq G$.

1. Update the proportion of intrinsic genes p from

$$\text{Beta} \left(a_p + \sum_{g=1}^G L_g, b_p + G - L_g \right).$$

2. Sample the variance of the spike component of the spike-and-slab prior $\tau_{\mu 0}^2$ from

$$\text{Inv}\Gamma\left(a_{\tau_{\mu 0}} + \frac{K}{2} \sum_{g=1}^G I(L_g = 0), b_{\tau_{\mu 0}} + \frac{1}{2} \sum_{\{(g,k):L_g=0\}} \mu_{gk}^2\right).$$

3. Sample the variance of the slab component of the spike-and-slab prior $\tau_{\mu 1}^2$ from

$$\text{Inv}\Gamma\left(a_{\tau_{\mu 1}} + \frac{K}{2} \sum_{g=1}^G I(L_g = 1), b_{\tau_{\mu 1}} + \frac{1}{2} \sum_{\{(g,k):L_g=1\}} \mu_{gk}^2\right).$$

4. Sample the variance of the guidance of non-intrinsic genes $\tau_{U_0}^2$ from

$$\text{Inv}\Gamma\left(a_{\tau_{U_0}} + \frac{1}{2} \sum_{g=1}^G I(L_g = 0), b_{\tau_{U_0}} + \frac{1}{2} \sum_{\{g:L_g=0\}} U_g^2\right).$$

5. Sample the variance of the guidance of intrinsic genes $\tau_{U_1}^2$ from

$$\text{Inv}\Gamma\left(a_{\tau_{U_1}} + \frac{1}{2} \sum_{g=1}^G I(L_g = 1), b_{\tau_{U_1}} + \frac{1}{2} \sum_{\{g:L_g=1\}} (U_g - 1)^2\right).$$

6. Update gene selection indicator L_g from the Bernoulli distribution

$$\text{Bern}\left(\frac{p \cdot \prod_{k=1}^K \text{N}(\mu_{gk}; 0, \tau_{\mu 1}^2) \cdot \text{N}(U_g; 1, \tau_{U_1}^2)}{p \cdot \prod_{k=1}^K \text{N}(\mu_{gk}; 0, \tau_{\mu 1}^2) \cdot \text{N}(U_g; 1, \tau_{U_1}^2) + (1-p) \cdot \prod_{k=1}^K \text{N}(\mu_{gk}; 0, \tau_{\mu 0}^2) \cdot \text{N}(U_g; 0, \tau_{U_0}^2)}\right).$$

7. Sample subtype proportion $\boldsymbol{\pi}$ from the Dirichlet distribution

$$\text{Dir}\left(c + \sum_{i=1}^n I(Z_i = 1), \dots, c + \sum_{i=1}^n I(Z_i = K)\right).$$

8. For each sample i , update its subtype indicator Z_i based on multinomial distribution

$$\text{Mult}(1; q_1, \dots, q_K),$$

where $q_k^* = \pi_k \exp\left\{-\sum_{g=1}^G \frac{(X_{gi} - \mu_{gk})^2}{2\sigma_g^2}\right\}$ and $q_k = \frac{q_k^*}{\sum_k q_k^*}$.

9. For each gene g and each subtype k , sample the mean of gene expression μ_{gk} from

$$\text{N}\left(\frac{\tau_{\mu L_g}^2 \sum_{i \in \{Z_i=k\}} X_{gi} \sigma_g^2}{\tau_{\mu L_g}^2 \cdot \sum_{i=1}^n I(Z_i = k) + \sigma_g^2}, \frac{\tau_{\mu L_g}^2 \sigma_g^2}{\tau_{\mu L_g}^2 \cdot \sum_{i=1}^n I(Z_i = k) + \sigma_g^2}\right),$$

where $\tau_{\mu L_g} = I(L_g = 1)\tau_{\mu 1} + I(L_g = 0)\tau_{\mu 0}$.

10. For each gene, sample the variance of gene expression σ_g^2 from

$$\text{Inv}\Gamma\left(a_\sigma + \frac{n}{2}, b_\sigma + \frac{1}{2} \sum_{i=1}^n (X_{gi} - \mu_{gZ_i})^2\right),$$

where $\mu_{gZ_i} = \mu_{g1}$ if $Z_i = 1$ and $\mu_{gZ_i} = \mu_{g0}$ if $Z_i = 0$.

2.3.6 Decision making

Denote N_T as the total number of iterations from the Gibbs sampling; N_B as the number of burn-in samples. The burn-in samples are discarded from the Bayesian inference because these initial samples may not necessarily converge to the stationary distribution of the full posterior likelihood (Equation 2.3.2). Throughout this manuscript, we set $N_T = 1000$ and $N_B = 500$, unless otherwise specified. After the Gibbs sampling, a total of $N = N_T - N_B$ posterior samples are used for further Bayesian inference.

To infer if a gene is an intrinsic gene (i.e., genes that contribute to separate the subtypes), we first denote Ω_I as the collection of intrinsic genes (i.e., $\Omega_I = \{g : 1 \leq g \leq G; \text{gene } g \text{ is an intrinsic gene}\}$), and $\Omega_{\bar{I}}$ as the collection of non-intrinsic genes (i.e., $\Omega_{\bar{I}} = \{g : 1 \leq g \leq G; g \notin \Omega_I\}$). We denote $P_g = \Pr(g \in \Omega_{\bar{I}} | L_g = 1) = 1 - \Pr(g \in \Omega_I | L_g = 1)$, which is also referred as the local false discovery rate (Efron and Tibshirani, 2002). Given a threshold η ($0 < \eta < 1$), we declare gene g as an intrinsic gene if $P_g \leq \eta$, and the expected number of false discoveries is $\sum_g P_g I(P_g \leq \eta)$. According to Newton et al. (2004), the resulting expected false discovery rate for genes with $P_g \leq \eta$, $1 \leq g \leq G$ is

$$\text{FDR}(\eta) = \frac{\sum_{g=1}^G P_g \cdot I(P_g \leq \eta)}{\sum_{g=1}^G I(P_g \leq \eta)}.$$

In practice, we will estimate P_g as $\frac{1}{N} \sum_{t=N_B+1}^{N_T} L_g^{[t]}$.

We infer the subtype for each subject i from the posterior samples of Z_i . A probabilistic assignment of sample i to cluster k can be calculated as

$$l_i^{(k)} = \frac{1}{N} \sum_{t=N_B+1}^{N_T} I(Z_i^{[t]} = k).$$

In our paper, we used the maximum a posteriori (MAP) estimation to decide the cluster assignment for sample i (i.e., $\arg \max_k l_i^{(k)}$). In our simulations and real data applications, we did not encounter any label switching problem (See trace plots in Figure S3-S6). This is probably because the clinical guidance help stabilize the clustering results and gene selections. In other scenarios, if there exists a label switching

problem, we would recommend methods by Robert (2007) and Stephens (2000) to tackle the label switching issue.

2.3.7 Extension to other types of clinical outcome variables

In Section 2.3.1, we used a gene specific guidance term U_g ($0 \leq U_g \leq 1$) to capture the association strength between gene g and a clinical outcome variable. If the clinical variable is continuous, U_g can be calculated as the absolute value of the Pearson correlation (ρ) between gene g and the clinical variable, or the coefficient of determination R^2 (R^2 is the same as the square of ρ) from a univariate linear regression model, where the dependent variable is the clinical variable and the independent variable is the expression level of gene g . In general, the clinical variable can be any data type, including continuous, binary, ordinal, count, survival, etc. We extend the linear regression model to a generic univariate regression model f_g to accommodate various types of clinical outcome variables. For example, generalized linear models can be used for binary, ordinal, and count data; Cox models can be used for survival data. Similar to the coefficient of determination R^2 , Cox and Snell (1989) proposed the pseudo R-squared for a generic univariate regression f_g :

$$R_g^2 = 1 - \left[\frac{L(f_0)}{L(f_g)} \right]^{2/n}$$

where n is the number of subjects; $L(f_0)$ is the likelihood of null model; and $L(f_g)$ is the likelihood of the model f_g . To ensure this term has the scale of $[0,1]$, we further proposed an adjusted pseudo R-squared:

$$U_g = \frac{R_g^2 - \min(R_g^2)}{\max(R_g^2) - \min(R_g^2)}$$

3 Result

In this section, we first evaluated the performance of the GuidedBayesianClustering using simulation datasets, and compared with the regular sparse Bayesian clustering method (the BayesianClustering, see Section 2). Further, we applied these methods in a gene expression profile of breast cancer to illustrate the superior performance of our proposed method. We benchmarked the performance in terms of both clustering performance and gene selection performance. For the clustering performance, we used adjusted Rand index (Hubert and Arabie, 1985) (ARI). ARI characterizes the consistency between a clustering assignment result and the underlying true clustering assignment, which ranges from -1 (indicating poor agreement) to 1 (indicating perfect agreement). For gene selection performance, we used the Jaccard index (Jaccard, 1901) to benchmark the similarity of the selected genes to the underlying intrinsic genes. Jaccard index is defined

as the ratio of the number of intersected genes appeared in both sets to the number of genes appeared in at least one gene set. The range for a Jaccard index is from 0 (indicating no overlap) to 1 (indicating fully overlap).

3.1 Simulation

3.1.1 Simulation setting

We simulated a gene expression study with $K = 3$ subtypes to evaluate the performance of the Guided-BayesianClustering and to compare with the BayesianClustering (i.e., the sparse Gaussian mixture model, Section 2.2). To mimic the multifaceted clustering configurations defined by different sets of genes, we simulated intrinsic genes which define disease-related subtype clusters, confounding impacted genes which define other configurations of clusters (non-disease-related), and noise genes (i.e., housekeeping genes). Correlated gene structures (Huo et al., 2016) were simulated for intrinsic genes and confounding impacted genes to best preserve the complex structure of genomic data. In addition, we generated a continuous outcome variable related to the intrinsic genes as the clinical guidance. Below is the detailed simulation data generation process.

(a) Intrinsic genes.

1. Simulate $K = 3$ disease-related subtypes. For each subtype $k(1 \leq k \leq K)$, simulate $N_k \sim \text{POI}(100)$ subjects, where POI denotes the Poisson distribution. The total number of subjects in the study is $N = \sum_k N_k$.
2. Simulate $M = 20$ gene modules. Denote n_m as the number of gene features in module m ($1 \leq m \leq M$). Sample $n_m \sim \text{POI}(20)$. Repeat this for all M modules, and on average there will be 400 intrinsic genes.
3. Denote the baseline level of subtype $k(1 \leq k \leq K)$ as θ_k ; and the template gene expression level of subtype k and module m as μ_{km} . The baseline level is set as $\theta_k = 2 + 2k$, and the template gene expression is calculated by $\mu_{km} = \alpha_m \theta_k + \text{N}(0, \sigma_0^2)$, where α_m is the fold change for each module m and $\alpha_m \sim \text{UNIF}((-2, -0.2) \cup (0.2, 2))$ and σ_0 is set to be 1.
4. Add biological variation σ_1^2 to the template gene expression μ_{km} such that $X'_{kmi} \sim \text{N}(\mu_{km}, \sigma_1^2)$, where $i(1 \leq i \leq N_k)$ is the subject index; k is the subtype index, and $m(1 \leq m \leq M)$ is the module index. We set σ_1 to be 3 unless otherwise specified.
5. Add correlation structure for genes in subtype k and module m . First sample $\Sigma'_{km} \sim \text{W}^{-1}(\phi, \nu)$, where $\phi = 0.5I_{n_m \times n_m} + 0.5J_{n_m \times n_m}$, $\nu = 60$, W^{-1} denotes the inverse Wishart distribution,

$I_{n_m \times n_m}$ is an n_m by n_m identity matrix and $J_{n_m \times n_m}$ is an n_m by n_m matrix with all elements equal to 1. The covariance matrix Σ_{km} is calculated by standardizing Σ'_{km} such that all the diagonal elements are equal to 1.

6. Simulate gene expression values for all genes in module m as $(X_{1kmi}, \dots, X_{n_mkmi})^\top \sim \text{MVN}(X'_{kmi}, \Sigma_{km})$, where $1 \leq k \leq K$, $1 \leq m \leq M$ and $1 \leq i \leq N_k$. MVN denotes the multivariate normal distribution.

(b) Phenotypic variables.

1. Simulate the continuous clinical outcome variable as $Y_{ki} \sim \text{N}(\theta_k, \sigma_2^2)$ for subject i in subtype k , where $1 \leq i \leq N_k$ and $1 \leq k \leq K$. We set σ_2 to be 6 so that the magnitude of U_g of the intrinsic genes in the simulation is comparable to that in the breast cancer example (See details in Section 3.2).

(c) Confounding impacted genes.

1. Simulate $V = 4$ confounding variables. Confounding variables could be gender, race, or other confounding factors. These variables will define subtype clusters driven by non-disease related genes, and thus complicate the process for disease subtype discovery. For each confounding variable v ($1 \leq v \leq V$), we similarly simulate $R = 20$ modules. For each module r_v ($1 \leq r_v \leq R$), similarly sample number of genes $n_{r_v} \sim \text{POI}(20)$. After repeating this procedure for all modules in all confounding variables, on average there will be 1,600 confounding impacted genes.
2. For each confounding variable v in the simulation, we randomly divided the N samples into K subclasses, which represents the non-disease-related clusters defined by confounding impacted genes.
3. Similar to Step a3, we denote θ_k as the baseline gene expression of subclass k ($1 \leq k \leq K$) for each confounding variable, and set $\theta_k = 2 + 2k$. Denote μ_{kr_c} as the template gene expression in subclass k ($1 \leq k \leq K$) and module r_c ($1 \leq r_c \leq 20$). We calculate the template gene expression by $\mu_{kr_c} = \alpha_{r_c} \theta_k + \text{N}(0, \sigma_0^2)$, where α_{r_c} is the fold change for each module r_c and $\alpha_{r_c} \sim \text{UNIF}((-2, -0.2) \cup (0.2, 2))$.
4. The biological variation σ_1^2 is added to the template gene expression such that $X'_{kr_c i} \sim \text{N}(\mu_{kr_c}, \sigma_1^2)$.
5. Following Step a5 and a6, we simulate gene correlation structure Σ_{km} within modules of confounder impacted genes, and generate their gene expression by $(X_{1kr_c i}, \dots, X_{n_mkr_c i})^\top \sim \text{MVN}(X'_{kr_c i}, \Sigma_{km})$.

(d) Noise genes.

1. We additionally simulate 3,000 noninformative noise genes (i.e., housekeeping genes) denoted by g . We generate template gene expression $\mu_g \sim \text{UNIF}(4, 8)$. Then, we add noise $\sigma_3 = 1$ to the template gene expression and generate $Y_{gi} \sim \text{N}(\mu_g, \sigma_3^2)$.

3.1.2 Simulation results

For the GuidedBayesianClustering, the clinical guidance term U_g was calculated as the adjusted pseudo R-squared (Section 2.3.7) from univariate linear regressions. We follow the description in Section 2.3.3 to set the hyper parameters unless otherwise specified. As shown in Figure 4a, the number of clusters was estimated as $K = 3$ via the BIC in Section 2.3.5. We controlled the FDR at 0.001 to select genes in both the GuidedBayesianClustering and the BayesianClustering.

Table 1 shows the comparison results of the two methods with the biological variation $\sigma_1 = 1$. Regarding clustering accuracy, the GuidedBayesianClustering (mean ARI = 0.985) outperformed the BayesianClustering (mean ARI = 0.142). In terms of gene selection, the GuidedBayesianClustering (mean Jaccard index = 0.864) outperformed the BayesianClustering (mean Jaccard index = 0.184). Since in this scenario, the Jaccard index represented the gene selection accuracy at a specific cutoff (i.e., FDR 0.001), it was unclear whether the superior performance of the GuidedBayesianClustering was related to this specific cutoff selection instead of the method itself. We thus further compared the gene selection performance by the area under the curve (AUC) of a ROC curve. To be specific, we iterated all possible FDR cutoffs and calculated their corresponding sensitivity and specificity for the accuracy of selecting the intrinsic genes. The AUC of this ROC curve (sensitivity by 1 - specificity) represented the overarching prediction power regardless of a specific FDR cutoff. Not surprisingly, the GuidedBayesianClustering (mean AUC = 0.984) achieved better performance than the BayesianClustering (mean AUC = 0.580). In addition, under the settings with varying biological variation ($\sigma_1 = 1$ to 5 with interval 0.5), Figure 4b and Figure 4c show that the GuidedBayesianClustering still outperformed the BayesianClustering in terms of both clustering and gene selection accuracy, though the performance of both methods decreased as the biological variation increased. The superior performance of the GuidedBayesianClustering is expected because it utilized the clinical outcome information to facilitate the identification of clinically related subtypes.

3.1.3 Sensitivity analysis

Since we assigned informative prior to $\tau_{\mu_0}^2$ and $\tau_{\mu_1}^2$ with hyper parameters $a_{\tau_{\mu_0}} = 2$, $b_{\tau_{\mu_0}} = 0.005$, $a_{\tau_{\mu_1}} = 4$, $b_{\tau_{\mu_1}} = 450$, we conducted sensitivity analysis to check the impacts of the choices of these hyper parameters on the clustering results and gene selection results. Each time, we varied one hyper parameter while fixing the other three hyper parameters. Specifically, we examined 10 evenly-spaced values from 1.1 to 2 for $a_{\tau_{\mu_0}}$; 10

Table 1: Comparison in the performance of clustering and gene selection between the GuidedBayesianClustering and the BayesianClustering with biological variation $\sigma_1 = 1$. Mean estimates and standard errors were reported based on $B = 100$ simulations. Clustering accuracy were evaluated by ARI. Gene selection accuracy were evaluated by Jaccard index and AUC.

	Clustering results		Gene selection results	
	ARI	Jaccard index	AUC	
GuidedBayesianClustering	0.985 (0.005)	0.864 (0.005)	0.984 (0.001)	
BayesianClustering	0.142 (0.014)	0.134 (0.011)	0.580 (0.013)	

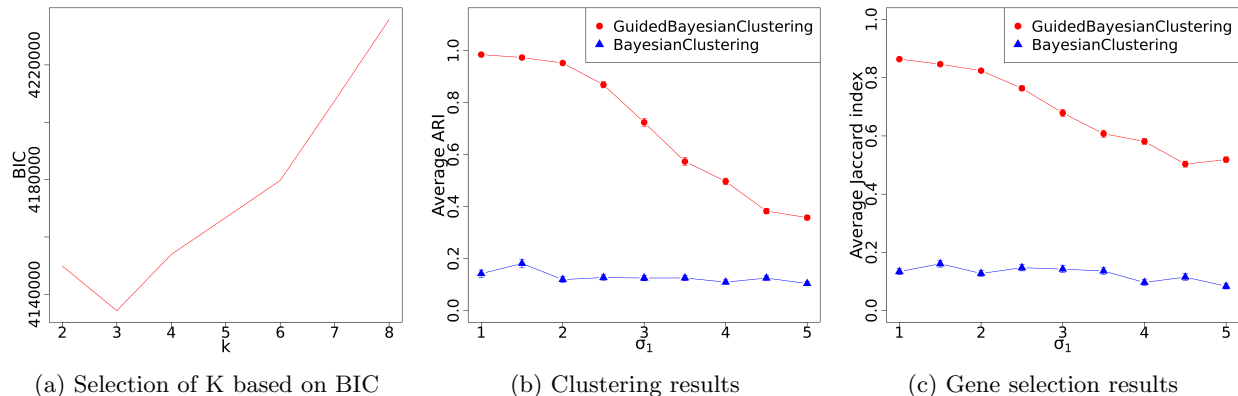


Figure 4: (a) Using BIC criteria for choosing the number of subtype K based on one simulation with biological variation $\sigma_1 = 1$; (b-c) the comparison between the GuidedBayesianClustering and the BayesianClustering with different values of biological variation σ_1 . Mean estimates were reported based on $B = 100$ simulations. (b) shows the clustering accuracy evaluated using ARI; (c) shows gene selection accuracy evaluated using Jaccard index.

evenly-spaced values from 0.0005 to 0.005 for $b_{\tau_{\mu_0}}$; 10 evenly-spaced values from 1.5 to 6 for $a_{\tau_{\mu_1}}$; 10 evenly-spaced values from 50 to 500 for $b_{\tau_{\mu_1}}$. As shown in Figure S1, the choices of the four hyper parameters have no effects on the clustering results. Figure S2 shows that the choices of the four hyper parameters have little effect on the gene selection results. Therefore, our algorithm is not sensitive to the perturbation of these informative hyper parameters, and we will stick with the proposed value of the informative hyper parameters throughout the article.

3.2 Breast cancer application

We examined the performance of the GuidedBayesianClustering in METABRIC, a breast cancer gene expression dataset (Curtis et al., 2012), which contains gene expression profile of 24,368 genes and 1,870 subjects. After filtering out 50% low expression genes based on the average expression level of each gene, scaling the data such that each gene has mean expression value 0 and standard deviation 1, we ended up with 12,180 gene features. Various types of clinical outcome variables existed in this cohort, including the Nottingham

prognostic index (NPI, continuous variable); Estrogen receptor status (ER, binary variable); HER2 receptor status (HER2, ordinal variable); and overall survival. Each of these 4 phenotypic variables was used as the clinical guidance for the GuidedBayesianClustering, respectively. We denote these methods as NPI-GuidedBayesianClustering, ER-GuidedBayesianClustering, HER2-GuidedBayesianClustering, and Survival-GuidedBayesianClustering.

Regarding each of these outcome variables, we calculated U_g as the coefficient of determination R^2 or adjusted pseudo- R^2 from the univariate regression between gene g and an outcome variable, where we applied the linear model on the continuous outcome; generalized linear models on the binary and ordinal outcome; and the Cox regression model on the survival outcome. We set the number of subtypes $K = 5$ since the PAM50 definition (Perou et al., 2000) implied there existed 5 subtypes of breast cancer. After 1,000 iterations for Gibbs sampling, we discarded the first 500 iterations as burn-in samples and keep the last 500 iterations for inference. To check the convergence of the parameters μ_{gk} , σ_g , $\tau_{\mu 0}$, $\tau_{\mu 1}$, τ_{U0} , and τ_{U1} , we drew trace plots for these parameters using sample after the burn-in period. As shown in Figure S3, (NPI-GuidedBayesianClustering), Figure S4 (ER-GuidedBayesianClustering), Figure S5 (HER2-GuidedBayesianClustering), and Figure S6 (Survival-GuidedBayesianClustering), all these parameters converge to their stationary distribution. For a fair comparison between the GuidedBayesianClustering and the non-guided BayesianClustering, we selected number of intrinsic genes to be exactly 400 for both methods (See Table 2), which can be achieved by adjusting the FDR criteria. This will help eliminate the possibility that the superior performance of a method is due to the more/less number of selected genes compared to the other method.

We used Silhouette score (Rousseeuw, 1987) to benchmark the homogeneity of subtype patterns. A larger Silhouette score indicates both better separation between clusters and better cohesion within respective clusters. For the heatmap patterns, the GuidedBayesianClustering achieved more homogenous clustering results (mean Silhouette = 0.053 ~ 0.071, Figure 5a, 5c, 5e, 5g) than the BayesianClustering (mean Silhouette = 0.037, Figure 5i). Since we did not have the underlying true clustering result, we further used the overall survival difference between subtypes to examine whether the resulting subtypes were clinically meaningful. The Kaplan-Meier survival curves of the five disease subtypes obtained from each GuidedBayesianClustering methods were well separated with highly significant p-values ($p = 7.3 \times 10^{-12} \sim 1.17 \times 10^{-8}$), Figure 5b, 5d, 5f, 5h), while the BayesianClustering method only achieved moderate significant survival difference ($p = 0.004$, Figure 5j). This is expected since all the GuidedBayesianClustering methods had guidance from clinical outcome variables but the BayesianClustering method did not. Remarkably, the NPI-GuidedBayesianClustering, the ER-GuidedBayesianClustering, and the HER2-GuidedBayesianClustering still achieved good survival separation even though they did not use any survival information. This is not un-

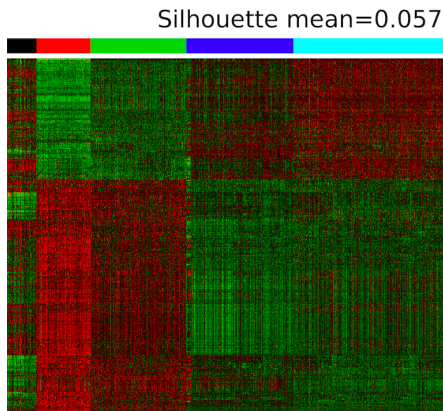
reasonable as all these clinical variables were related to the breast cancer and thus could impact the overall survival.

We further evaluated the clustering results obtained from each method by comparing with PAM50 subtypes, which is regarded as the gold standard for breast cancer subtypes. Table 2 shows that the ARI values from four types of GuidedBayesianClustering (0.233 ~ 0.236) were greater than the ARI values from the BayesianClustering (0.177), indicating that the subtype results from the GuidedBayesianClustering were closer to the gold standard than those from the BayesianClustering.

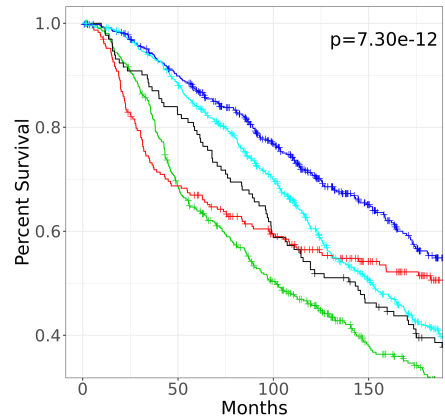
Table 2: Comparison in clustering and gene selection of the four GuidedBayesianClustering methods and the non-guided BayesianClustering method. The number of genes selected by each method was 400. The clustering results were compared with PAM50 subtype in terms of ARI. The separation between resulting clusters and cohesion in respective clusters were evaluated by the mean Silhouette score. P-values of survival differences of identified subgroups were calculated based on the log-rank test.

Method	Guidance	Genes	ARI	Silhouette	p-value
Guided BayesianClustering	NPI(continuous)	400	0.234	0.057	7.30×10^{-12}
	ER(binary)	400	0.234	0.062	1.65×10^{-10}
	HER2(ordinal)	400	0.233	0.053	3.26×10^{-12}
	Survival	400	0.236	0.071	1.17×10^{-8}
BayesianClustering		400	0.177	0.037	0.004

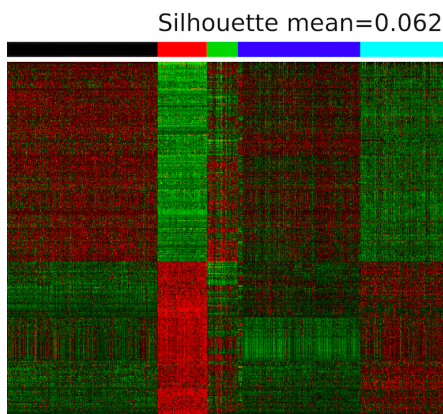
To evaluate whether the selected genes were biologically meaningful, we performed pathway enrichment analysis via the BioCarta pathway database using the Fisher’s exact test. Figure 6 shows the enriched pathways obtained from each method using. Using $p = 0.05$ as cutoff, the number of significant pathways obtained from the NPI-GuidedBayesianClustering (n=8), the ER-GuidedBayesianClustering (n=13), the HER2-GuidedBayesianClustering (n=8) and the Survival-GuidedBayesianClustering (n=9) were more than that obtained from the BayesianClustering (n=3). This means the genes selected by the GuidedBayesianClustering methods with four clinical outcome variables were more biologically interpretable than those selected by the non-guided BayesianClustering method. Notably, the genes selected by the ER-GuidedBayesianClustering and the HER2-GuidedBayesianClustering were enriched in HER2 pathway, with $p = 1.69 \times 10^{-3}$, and $p = 0.011$ respectively. This is consistent with previous research that ER signaling pathway and HER2 signaling pathway are closely related to breast cancer (Giuliano et al., 2013). In addition, the NPI-GuidedBayesianClustering and the ER-GuidedBayesianClustering identified ATRBRCA pathway as significant with both $p = 9.65 \times 10^{-3}$, which has been found closely related to breast cancer susceptibility (Paul and Paul, 2014). In contrast, these hallmark pathways of breast cancer were not picked up by the BayesianClustering method. Therefore, the GuidedBayesianClustering methods have the capability of selecting the most biologically interpretable genes.



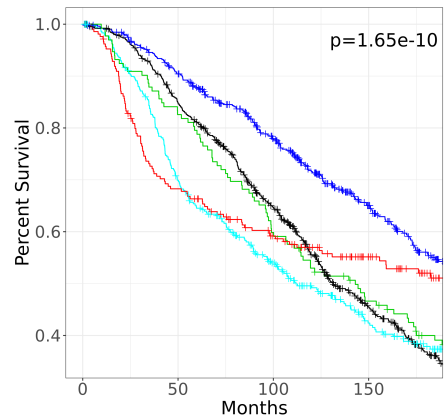
(a) Heatmap from the NPI-GuidedBayesianClustering



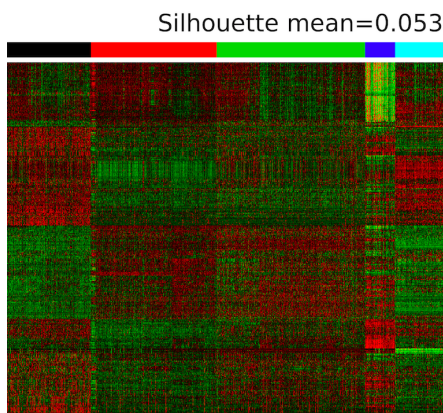
(b) Survival curves from NPI-GuidedBayesianClustering



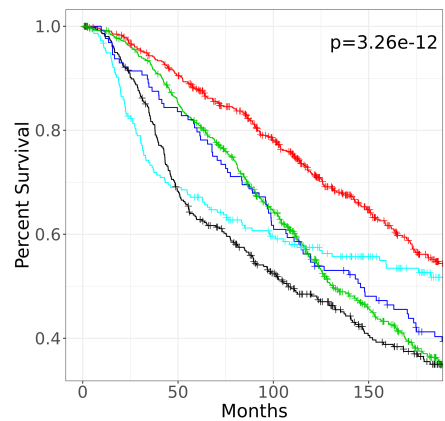
(c) Heatmap from ER-GuidedBayesianClustering



(d) Survival curves from ER-GuidedBayesianClustering



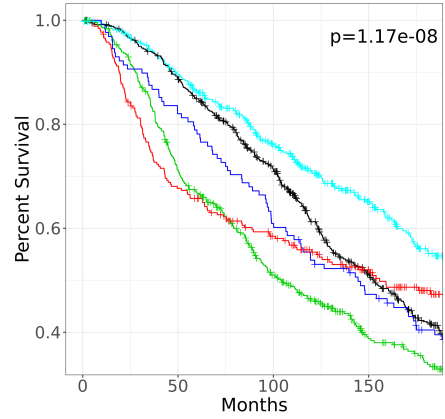
(e) Heatmap from HER2-GuidedBayesianClustering



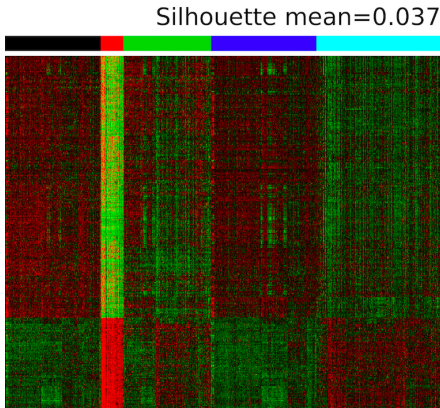
(f) Survival curves from HER2-GuidedBayesianClustering



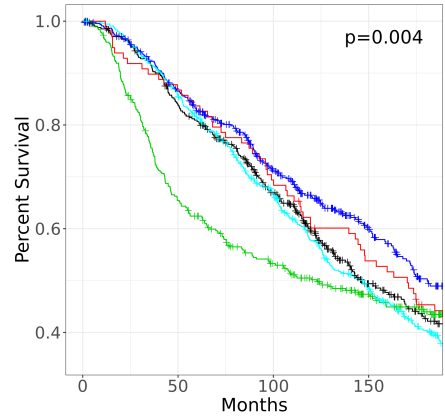
(g) Heatmap from Survival-GuidedBayesianClustering



(h) Survival curves from Survival-GuidedBayesianClustering



(i) Heatmap from BayesianClustering



(j) Survival curves from BayesianClustering

Figure 5: Gene expression heatmap and Kaplan–Meier survival curve of the METABRIC dataset using the NPI-GuidedBayesianClustering, the ER-GuidedBayesianClustering, the HER2-GuidedBayesianClustering, the Survival-GuidedBayesianClustering and the BayesianClustering. In heatmap (a)(c)(e)(g)(i), rows represent genes and columns represent samples. Red color represents higher expression and green color represents lower expression. The samples are divided into 5 clusters with 5 colors in the bar above the heatmaps. In survival curves (b)(d)(f)(h)(j), the color of the survival curve for each subtype is corresponding to the subtype color in the heatmap of the same method.

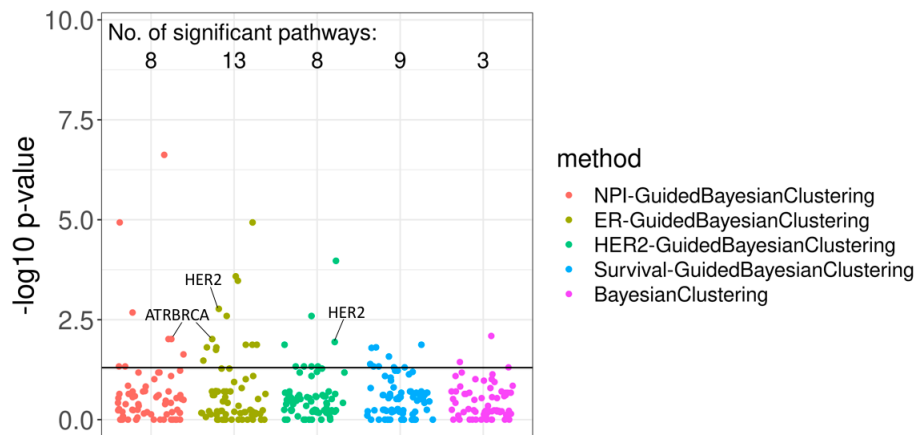


Figure 6: Pathway enrichment analysis results for the GuidedBayesianClustering with four different types of guidance, the BayesianClustering. The number of significant pathways ($p < 0.05$) for each method is on the top.

4 Discussion

We proposed a full a Bayesian framework to identify disease subtypes via high-dimensional transcriptomic data. Our method is capable of performing gene selection, incorporating the guidance from a clinical outcome variable. Various types of clinical outcome variables, including continuous, binary, ordinal and survival data, could be incorporated as guidance in our framework. Conjugate priors were employed to facilitate the efficient Gibbs sampling. A decision framework was implemented to infer the false discovery rate of the selected genes. Through simulations as well as breast cancer gene expression data application, we demonstrated that our proposed method (i.e., the GuidedBayesianClustering method) was superior to the non-guided method (i.e., BayesianClustering method) in terms of both clustering accuracy and gene selection accuracy/interpretability.

Since our method can only accommodate one clinical outcome variable, one issue is how to properly select the clinical guidance given multiple available clinical outcomes. If there exist domain knowledges, we suggest to select the outcome variable of the most biological interest as clinical guidance. On the other hand, if no domain knowledge can be used or one prefers a data driven approach, we suggest to try several outcome variables as guidance, and decide the best outcome guidance based on the biological interpretability of the clustering results (i.e., survival difference, pathway analysis). In our breast cancer application example, we would recommend to use the result from ER-GuidedBayesianClustering because of its (i) good subtype pattern; (ii) significant survival difference between subtypes; and (iii) most number of significant enriched pathways. To further address this issue, we will develop a multivariate outcome-guided Bayesian clustering method in the future, which will incorporate multiple outcome variables as the clinical guidance. With the

accumulation of high-dimensional omics data and their relevant clinical outcomes, our proposed method will be quite applicable to identify clinically meaningful disease subtypes.

References

- Bair, E. and Tibshirani, R. (2004). Semi-supervised methods to predict patient survival from gene expression data. *PLoS biology*, 2(4):e108.
- Basu, S., Banerjee, A., and Mooney, R. J. (2004). Active semi-supervision for pairwise constrained clustering. In *Proceedings of the 2004 SIAM international conference on data mining*, pages 333–344. SIAM.
- Bouveyron, C. and Brunet-Saumard, C. (2014). Model-based clustering of high-dimensional data: A review. *Computational Statistics & Data Analysis*, 71:52–78.
- Bredesen, D. E. (2015). Metabolic profiling distinguishes three subtypes of alzheimer’s disease. *Aging*, 7(8):595–600.
- Coates, A., Winer, E., Goldhirsch, A., Gelber, R., Gnant, M., Piccart-Gebhart, M., Thürlimann, B., Senn, H.-J., André, F., Baselga, J., Bergh, J., Bonnefoi, H., Burstein, H., Cardoso, F., Castiglione-Gertsch, M., Coates, A. S., Colleoni, M., Curigliano, G., Davidson, N. E., Di Leo, A., Ejlertsen, B., Forbes, J. F., Galimberti, V., Gelber, R. D., Gnant, M., Goldhirsch, A., Goodwin, P., Harbeck, N., Hayes, D. F., Huober, J., Hudis, C. A., Ingle, J. N., Jassem, J., Jiang, Z., Karlsson, P., Morrow, M., Orecchia, R., Kent Osborne, C., Partridge, A. H., de la Peña, L., Piccart-Gebhart, M. J., Pritchard, K. I., Rutgers, E. J., Sedlmayer, F., Semiglazov, V., Shao, Z.-M., Smith, I., Thürlimann, B., Toi, M., Tutt, A., Viale, G., von Minckwitz, G., Watanabe, T., Whelan, T., Winer, E. P., and Xu, B. (2015). Tailoring therapies—improving the management of early breast cancer: St gallen international expert consensus on the primary therapy of early breast cancer 2015. *Annals of Oncology*, 26(8):1533 – 1546.
- Cox, D. and Snell, E. (1989). *Analysis of Binary Data*, volume 32. CRC Press.
- Curtis, C., Shah, S. P., Chin, S.-F., Turashvili, G., Rueda, O. M., Dunning, M. J., Speed, D., Lynch, A. G., Samarajiwa, S., Yuan, Y., et al. (2012). The genomic and transcriptomic architecture of 2,000 breast tumours reveals novel subgroups. *Nature*, 486(7403):346.
- Dudoit, S. and Fridlyand, J. (2002). A prediction-based resampling method for estimating the number of clusters in a dataset. *Genome Biology*, 3(7):1–21.

- Efron, B. and Tibshirani, R. (2002). Empirical bayes methods and false discovery rates for microarrays. *Genetic epidemiology*, 23(1):70–86.
- Eisen, M. B., Spellman, P. T., Brown, P. O., and Botstein, D. (1998). Cluster analysis and display of genome-wide expression patterns. *Proceedings of the National Academy of Sciences*, 95(25):14863–14868.
- Gaynor, S. and Bair, E. (2017). Identification of relevant subtypes via preweighted sparse clustering. *Computational statistics & data analysis*, 116:139–154.
- Geman, S. and Geman, D. (1984). Stochastic relaxation, gibbs distributions, and the bayesian restoration of images. *IEEE Transactions on pattern analysis and machine intelligence*, (6):721–741.
- Giuliano, M., Trivedi, M. V., and Schiff, R. (2013). Bidirectional crosstalk between the estrogen receptor and human epidermal growth factor receptor 2 signaling pathways in breast cancer: molecular basis and clinical implications. *Breast Care*, 8(4):256–262.
- Hubert, L. and Arabie, P. (1985). Comparing partitions. *Journal of classification*, 2(1):193–218.
- Huo, Z., Ding, Y., Liu, S., Oesterreich, S., and Tseng, G. (2016). Meta-analytic framework for sparse k-means to identify disease subtypes in multiple transcriptomic studies. *Journal of the American Statistical Association*, 111(513):27–42.
- Huo, Z., Tseng, G., et al. (2017). Integrative sparse k -means with overlapping group lasso in genomic applications for disease subtype discovery. *The Annals of Applied Statistics*, 11(2):1011–1039.
- Ishwaran, H., Rao, J. S., et al. (2005). Spike and slab variable selection: frequentist and bayesian strategies. *Annals of statistics*, 33(2):730–773.
- Jaccard, P. (1901). Étude comparative de la distribution florale dans une portion des alpes et des jura. *Bull Soc Vaudoise Sci Nat*, 37:547–579.
- Lehmann, B. D., Bauer, J. A., Chen, X., Sanders, M. E., Chakravarthy, A. B., Shyr, Y., and Pietenpol, J. A. (2011). Identification of human triple-negative breast cancer subtypes and preclinical models for selection of targeted therapies. *The Journal of clinical investigation*, 121(7):2750.
- Luo, X. and Wei, Y. (2019). Batch effects correction with unknown subtypes. *Journal of the American Statistical Association*, 114(526):581–594.
- McLachlan, G. J., Bean, R., and Peel, D. (2002). A mixture model-based approach to the clustering of microarray expression data. *Bioinformatics*, 18(3):413–422.

- Newton, M. A., Noueiry, A., Sarkar, D., and Ahlquist, P. (2004). Detecting differential gene expression with a semiparametric hierarchical mixture method. *Biostatistics*, 5(2):155–176.
- Nowak, G. and Tibshirani, R. (2008). Complementary hierarchical clustering. *Biostatistics*, 9(3):467–483.
- Pan, W. and Shen, X. (2007). Penalized model-based clustering with application to variable selection. *Journal of Machine Learning Research*, 8(May):1145–1164.
- Parker, J. S., Mullins, M., Cheang, M. C., Leung, S., Voduc, D., Vickery, T., Davies, S., Fauron, C., He, X., Hu, Z., et al. (2009). Supervised risk predictor of breast cancer based on intrinsic subtypes. *Journal of clinical oncology*, 27(8):1160–1167.
- Parsons, D. W., Jones, S., Zhang, X., Lin, J. C.-H., Leary, R. J., Angenendt, P., Mankoo, P., Carter, H., Siu, I.-M., Gallia, G. L., et al. (2008). An integrated genomic analysis of human glioblastoma multiforme. *Science*, 321(5897):1807–1812.
- Paul, A. and Paul, S. (2014). The breast cancer susceptibility genes (brca) in breast and ovarian cancers. *Frontiers in bioscience (Landmark edition)*, 19:605.
- Perou, C. M., Sørlie, T., Eisen, M. B., van de Rijn, M., Jeffrey, S. S., Rees, C. A., Pollack, J. R., Ross, D. T., Johnsen, H., Akslen, L. A., et al. (2000). Molecular portraits of human breast tumours. *Nature*, 406(6797):747–752.
- Prat, A., Pineda, E., Adamo, B., Galván, P., Fernández, A., Gaba, L., Díez, M., Viladot, M., Arance, A., and Muñoz, M. (2015). Clinical implications of the intrinsic molecular subtypes of breast cancer. *The Breast*, 24:S26–S35.
- Robert, C. (2007). *The Bayesian choice: from decision-theoretic foundations to computational implementation*. Springer Science & Business Media.
- Robert, C. and Casella, G. (2013). *Monte Carlo statistical methods*. Springer Science & Business Media.
- Rosenwald, A., Wright, G., Chan, W. C., Connors, J. M., Campo, E., Fisher, R. I., Gascoyne, R. D., Muller-Hermelink, H. K., Smeland, E. B., Giltnane, J. M., et al. (2002). The use of molecular profiling to predict survival after chemotherapy for diffuse large-b-cell lymphoma. *New England Journal of Medicine*, 346(25):1937–1947.
- Rousseeuw, P. J. (1987). Silhouettes: a graphical aid to the interpretation and validation of cluster analysis. *Journal of computational and applied mathematics*, 20:53–65.

- Sadanandam, A., Lyssiotis, C. A., Homicsko, K., Collisson, E. A., Gibb, W. J., Wullschleger, S., Ostos, L. C. G., Lannon, W. A., Grotzinger, C., Del Rio, M., et al. (2013). A colorectal cancer classification system that associates cellular phenotype and responses to therapy. *Nature medicine*, 19(5):619–625.
- Schwarz, G. et al. (1978). Estimating the dimension of a model. *Annals of statistics*, 6(2):461–464.
- Stephens, M. (2000). Dealing with label switching in mixture models. *Journal of the Royal Statistical Society: Series B (Statistical Methodology)*, 62(4):795–809.
- Tothill, R. W., Tinker, A. V., George, J., Brown, R., Fox, S. B., Lade, S., Johnson, D. S., Trivett, M. K., Etemadmoghadam, D., Locandro, B., et al. (2008). Novel molecular subtypes of serous and endometrioid ovarian cancer linked to clinical outcome. *Clinical Cancer Research*, 14(16):5198–5208.
- Van't Veer, L. J., Dai, H., Van De Vijver, M. J., He, Y. D., Hart, A. A., Mao, M., Peterse, H. L., Van Der Kooy, K., Marton, M. J., Witteveen, A. T., et al. (2002). Gene expression profiling predicts clinical outcome of breast cancer. *nature*, 415(6871):530–536.
- Verhaak, R. G., Hoadley, K. A., Purdom, E., Wang, V., Qi, Y., Wilkerson, M. D., Miller, C. R., Ding, L., Golub, T., Mesirov, J. P., et al. (2010). Integrated genomic analysis identifies clinically relevant subtypes of glioblastoma characterized by abnormalities in *PDGFRA*, *IDH1*, *EGFR*, and *NF1*. *Cancer cell*, 17(1):98–110.
- Vogenberg, F. R., Barash, C. I., and Pursel, M. (2010). Personalized medicine: part 1: evolution and development into theranostics. *Pharmacy and Therapeutics*, 35(10):560.
- Von Minckwitz, G., Untch, M., Blohmer, J.-U., Costa, S. D., Eidtmann, H., Fasching, P. A., Gerber, B., Eiermann, W., Hilfrich, J., Huober, J., et al. (2012). Definition and impact of pathologic complete response on prognosis after neoadjuvant chemotherapy in various intrinsic breast cancer subtypes. *J Clin Oncol*, 30(15):1796–1804.
- Williams-Gray, C. H. and Barker, R. A. (2017). parkinson disease: Defining pd subtypesâ a step toward personalized management? *Nature Reviews Neurology*, 13(8).
- Witten, D. M. and Tibshirani, R. (2010). A framework for feature selection in clustering. *Journal of the American Statistical Association*, 105(490):713–726.
- Xie, B., Pan, W., Shen, X., et al. (2008). Penalized model-based clustering with cluster-specific diagonal covariance matrices and grouped variables. *Electronic Journal of Statistics*, 2:168–212.